Optimization of a wall-less Hall thruster

Julien Vaudolon, Stéphane Mazouffre, Carole Hénaux, Dominique Harribey, and Alberto Rossi

Citation: Applied Physics Letters **107**, 174103 (2015); doi: 10.1063/1.4932196
View online: http://dx.doi.org/10.1063/1.4932196
View Table of Contents: http://scitation.aip.org/content/aip/journal/apl/107/17?ver=pdfcov
Published by the AIP Publishing

Optimization of a wall-less Hall thruster

Julien Vaudolon,[1,a)] Stéphane Mazouffre,[1] Carole Hénaux,[2] Dominique Harribey,[2] and Alberto Rossi[2]
[1]*ICARE - CNRS, 1C Avenue de la Recherche Scientifique, Orléans, France*
[2]*LAPLACE - CNRS, 2 rue Charles Camichel, Toulouse, France*

(Received 17 July 2015; accepted 16 September 2015; published online 27 October 2015)

An experimental optimization of a Hall thruster in wall-less operation mode is performed with the PPS-Flex, a 1.5 kW class thruster capable of modifying the magnetic field topology over a broad range of configurations. The anode geometry and the magnetic topology have been modified to avoid interaction between the magnetic field lines and the anode surface, compared to the first wall-less Hall thruster prototype. The measurements of the thrust and far-field ion properties reveal that a satisfactory performance level can be obtained once the magnetic barrier is restored, and pave the way towards the development of a high-efficiency wall-less Hall thruster. © *2015 AIP Publishing LLC*. [http://dx.doi.org/10.1063/1.4932196]

Hall thrusters (HTs) are advanced and mature propulsion devices primarily used for station-keeping and attitude control of geosynchronous communication satellites.[1,2] Recently, the launch of two satellites based on an all-electric bus has marked the debut of a new era. Several satellites are expected to reach operational orbit in the coming years using plasma thrusters instead of chemical engines for the orbit transfer maneuver.

HTs are efficient gridless ion accelerators with a long flight heritage. Their operating principle relies on the creation of a low-pressure quasi-neutral plasma discharge in a crossed magnetic and electric field configuration, in which a propellant gas, typically xenon, is ionized and accelerated.[3,4] In the standard configuration, the magnetized discharge is confined to an annular dielectric cavity with the anode at one end, where the gas is injected, and an external cathode that also serves as a beam neutralizer. Ionization of the propellant gas occurs inside the cavity. Ions are accelerated through a potential drop that stretches from the interior to the exterior of the cavity. Compared to gridded ion engines, Hall thrusters produce a moderate specific impulse but they furnish a large thrust-to-power ratio, which makes them preferable for orbit transfers.

The main drawback of conventional HTs is the fact that the wall material determines to a large extent the discharge properties, and consequently, the performance level, as well as the operational lifetime. The wall material plays a role in the plasma properties, through, among other effects, secondary electron emission. In addition, plasma-wall interaction generates power losses and thermal stress on the structure components. The erosion of the dielectric annular channel walls is mostly due to bombardment by high-energy ions.[5,6] The large particle flux towards the walls is a direct consequence of the magnetic field topology. In a HT, the accelerating electric field originates in a decrease of the electron mobility at the channel exit. An efficient barrier requires a radial magnetic field, the lines of which intersect the walls. Recently, an original approach to significantly reducing the erosion rate, hence prolonging the thruster lifetime, has been proposed and validated. This approach is termed magnetic shielding (MS).[7–12] MS consists in preventing the magnetic field lines from crossing the walls in the acceleration region. Instead, the lines remain parallel to the wall of the downstream section of the channel and they extend to the anode region to capture cold electrons. Such a topology strongly reduces the magnitude of the radial electric field component, thereby decreasing wall material sputtering.

There is another, more drastic alternative to limit interaction between the plasma and the surface in a HT. The principle is to shift the ionization and acceleration regions outside the cavity. This unconventional design was named a Wall-Less Hall Thruster, or WLHT in short.[13,14] In a WL thruster, the anode is moved to the exit plane of the dielectric channel. As shown in a recent work, the electric field is entirely shifted outside the cavity, in a region where the magnetic field gradient is negative.[13] A wall-less ion source provides an ideal platform for the study of cross-field discharge configurations with sophisticated tools like coherent and incoherent Thomson scattering and LIF spectroscopy. The access it provides to key regions of the plasma facilitates a thorough investigation of plasma instabilities and small-scale turbulence for a better understanding of the discharge physics and anomalous electron transport. Additionally, it allows to study these phenomena without the influence of wall processes such as secondary electron emission. On a more technological standpoint, it was demonstrated that the magnetized discharge can be moved outside the cavity without significantly compromising the ion production and acceleration. This study nonetheless revealed deterioration of the performance as well as weak points in the wall-less configuration: the beam energy is low, the plume divergence angle is large, and the discharge current is high.

Figure 1 (left) illustrates the interaction between the anode and the magnetic field lines in the basic configuration of the first WL Hall thruster low-power prototype. The magnetic circuit of this thruster was based on that of a classical Hall thruster. Therefore, the **B**-field lines are perpendicular to the thruster axis and they intercept the anode that is placed

a)julien.vaudolon@cnrs-orleans.fr

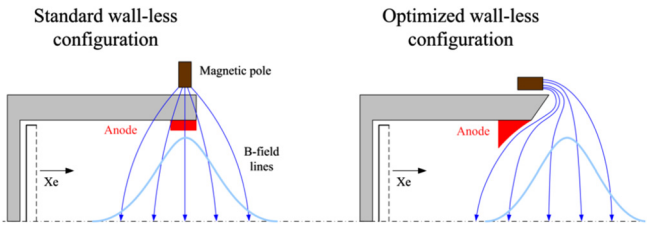

FIG. 1. (Left) Basic configuration of a wall-less Hall thruster: the anode is simply moved at the channel exit plane. The magnetic field lines intercept the anode. (Right) Optimized wall-less design: the magnetic field lines are parallel to the anode.

at the channel exhaust. The magnetic confinement thus becomes much less efficient. A large fraction of hot electrons originating from the external cathode and trapped along magnetic field lines are directly lost at the anode. The discharge current is therefore high and the ionization degree is low.

In order to prevent electron losses at the anode, the magnetic barrier must be restored. The basic idea is to make the magnetic field lines parallel to the anode surface. The anode could be rotated at 90° without changing the magnetic topology. This design is, however, not efficient for two reasons: (i) a large fraction of the magnetic flux is injected into the channel and it does not play any role in the electron trapping and thrust production and (ii) the magnetized region, where ionization and acceleration take place, is short, i.e., the number of electron-atom collision events is rather low. Figure 1 (right) portrays a more suitable design. The magnetic barrier is located in front of the channel exit plane by injecting the magnetic flux in the axial direction. The peak of the magnetic field is then shifted outside the cavity. The anode is still placed at the channel exhaust, but its shape is curved to avoid any interaction with the magnetic field lines: the lines never cross the anode surface. The optimized WL magnetic topology resembles the MS topology.[7–11] There is nevertheless one main difference. The magnetic field lines do not have to extend deep into the channel to capture cold electrons. This difference makes easier the generation of a WL topology by means of a magnetic circuit compared to a MS topology.

The optimization of the WLHT has been investigated with the PPS-Flex Hall thruster,[15,16] at PIVOINE-2g ground test facility. The PPS-Flex thruster is a 1.5 kW-class Hall thruster based on Snecma's PPS®1350 thruster architecture. It is a unique prototype in terms of magnetic flexibility. The circuit of the PPS-Flex has been especially designed to control in an independent manner all the characteristic parameters of a magnetic topology. The PPS-Flex is composed of 22 coils: 4 internal coils; 4 external stages, each with 4 coils connected in series, and two back coils. Experiments have been performed with the second version of the PPS-Flex thruster. This new version is fitted with additional heat pipes and with 8 large external radiators to reach a high input power level without damaging the magnetizing coils and the circuit. Recently, the PPS-FLEX was shown to be able to generate a MS-type topology in its actual magnetic design, which demonstrates its high magnetic flexibility.[12] The thruster has been fired up to 2 kW without troubles. In WL configuration, the PPS-Flex has been equipped with a curved anode split in two parts. The inner and outer rings are located at the exit plane of the straight section of the BN-SiO_2 channel and connected to one another.[14] The magnetic topology has been tuned and optimized during the experiments. The typical topology is given in Figure 1. The anode geometry and the magnetic map have been optimized to reach a high thrust efficiency. The discharge current drastically decreased when switching from a standard magnetic map to a WL map, as expected. Several quantities have been acquired: the thrust, the discharge current time series, the ion current density profile and the thruster component temperature by means of calibrated infrared thermal imaging.[6,17] The thruster was operated over of broad range of parameters: discharge voltage U_d from 200 V up to 500 V, anode flow rate ϕ_a between 2.0 mg/s and 3.5 mg/s of xenon, and input power ranging between 400 W and 1,500 W. A heated hollow cathode with a LaB_6 insert was used with a constant xenon mass flow rate of 0.4 mg/s. The cathode and the thruster body were floating but unbound.

The performance level of the PPS-Flex thruster in WL mode has been determined from thrust and ion current measurements. The ion current density profile was acquired in the plume far-field by means of a Faraday cup. The cup material was molybdenum to minimize the secondary electron emission yield. The cup length was 28 mm. A 16 mm in diameter entrance collimator made of graphite defines the collection solid angle and the ion collection geometrical area. The cup was biased at −49 V for all experimental conditions. The Faraday probe was installed on a rotating arm. The ion current was collected in the horizontal plane that includes the thruster axis from −90° to 90° with an angular step of 1°.

Several relevant quantities can be assessed from the data. The ion beam current is inferred from the ion current density profile j_i, measured at $R = 70$ cm downstream of the thruster exit plane, using Equation (1), in which θ is the co-latitude angle and ϕ the longitude angle.

$$I_b = R^2 \int_0^{\pi} \int_0^{\pi} j_i(\theta, \phi) \sin(\theta) d\theta d\phi. \quad (1)$$

The ionization efficiency, η_i, also termed propellant utilization, was obtained using Equation (2), which assumes the presence of singly charged ions only. The terms m_i and e stand for the ion mass and elementary charge, respectively,

$$\eta_i = \frac{m_i I_b}{e\phi_a}. \quad (2)$$

The anode efficiency η_a is computed from the thrust T using Equation (3), in which the power dissipated into the cathode and the coils is not considered

$$\eta_a = \frac{T^2}{2\phi_a U_d I_d}. \quad (3)$$

The stability of the discharge has been verified by operating the thruster in optimized WL mode at 300 V and 3.0 mg/s during 1 h. The discharge current reached a steady state at 2.75 A with a standard deviation of 0.4 A after 30 min. The curved anode was able to sustain the thermal load. Infrared thermal imaging did not reveal the formation of hot zones.

The discharge current waveforms measured on the anode line at 250 V and 3.0 mg/s are presented in Figure 2 in the standard (S), MS, and WL configurations. As in a conventional Hall thruster, the current trace of a thruster with an external discharge exhibits low-frequency oscillations from 10 to 30 kHz that correspond to the well-known breathing mode.[18] Such oscillations, which find their origin in an ionization instability, can be interpreted in terms of a predator-prey type of mechanism between atoms and ions.[18,19] Also shown in Figure 2 are the frequency spectra associated with the discharge current time series. These spectra are obtained using the Hilbert-Huang transform, which is well-suited for non-stationary signals.[20] The thruster design does not seem to modify the order of magnitude of the breathing mode frequency, nor the fact that it dominates the frequency spectrum energy content, two indications that the main physical processes that govern ionization in the cross-field discharge remain unchanged. The power spectra also show oscillations around 100 kHz in the standard and MS configurations. These oscillations encompass phenomena such as rotating and ion transit time instabilities.[19] These oscillatory phenomena are absent, or at least much weaker, in WLHT whatever the operating conditions. This observation on the PPS-Flex is similar to that made on our first WLHT prototype,[13] meaning this phenomenon is independent of the thruster size and power level.

Discharge current values are displayed in Figure 3 as a function of the applied voltage for 3 values of the xenon mass flow rates for an optimized WL configuration. The discharge current mean intensity is on the order of the injected mass flow rate, as expected. However, the discharge oscillation level is relatively high, especially above 300 V. The oscillation level corresponds to the standard deviation of the current time series. It therefore images the magnitude of the breathing oscillation.[18] The characteristics in WL mode are close to those obtained with the SPT100 topology. The MS topology always results in higher discharge current mean value and oscillation amplitude. Figure 3 also shows the ionization efficiency and beam divergence angle. The total ion current is quite large. Whatever the operating point, the ratio of the ion current to the discharge current is above 0.6. As a consequence, the ionization efficiency is high, with a peak value at 300 V. The ion beam divergence half-angle is large, above standard values. The strong divergence certainly originates in the fact the electric field is shifted downstream the channel exhaust, therefore making the electrostatic lens effect less efficient for focusing. The thrust level is deemed acceptable, given the current development level of the WL design. The anode efficiency presented in Figure 3 reaches acceptable values while the xenon mass flow rate is relatively low for a 1.5 kW device. Its magnitude is in fact not far from standard values for a high-efficiency Hall thruster with a classical design: 36% in WL vs 43% for a SPT100 topology. Notice the highest efficiency is reached at 300 V, for $\phi_a = 2.5$ and 3.0 mg/s. The specific impulse, ion current, and current utilization can be inferred from the data presented in Figure 3.

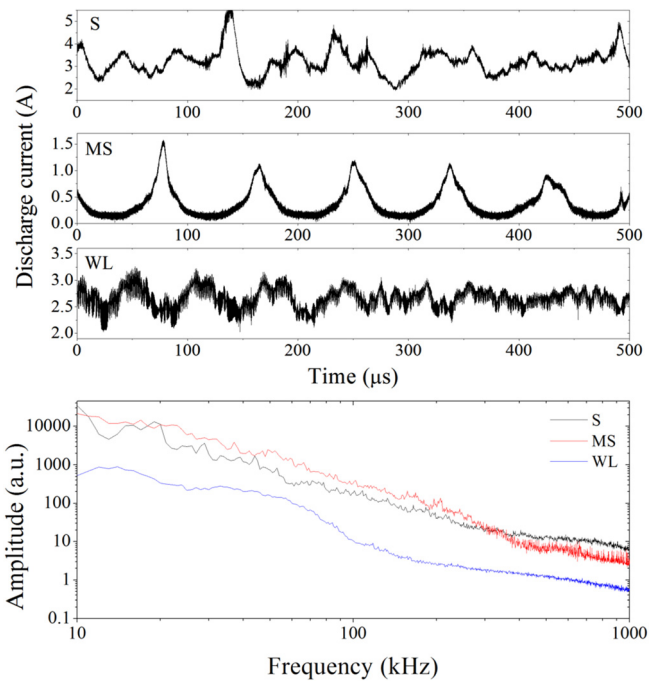

FIG. 2. (Top) Discharge current waveforms of the thruster in the standard (S), magnetic shielding (MS), and wall-less (WL) configurations, at 250 V and 3.0 mg/s of anode xenon flow rate. (Bottom) Corresponding frequency spectra computed using the Hilbert-Huang transform.

As demonstrated with the testing of the first wall-less Hall thruster prototype, the performance characteristics are degraded in simple wall-less configuration especially the discharge current and the ionization degree.[13] This study therefore aimed at optimizing the WLHT design by adapting the anode geometry and the magnetic topology. The strategy consists in avoiding the intersection between the anode and the magnetic field flux lines in order to prevent short-circuiting the magnetic barrier. Experiments have been carried out with the 1.5 kW-class PPS-Flex Hall thruster. Shaping the anode and adjusting the magnetic topology in parallel allows to strongly reduce the discharge current, to increase the propellant utilization and to achieve satisfactory thrust level, specific impulse, and anode efficiency. The thruster was operated up to 500 V. However, the current magnetic design does not allow the generation of WL configurations with a peak magnetic field above 90 G, which clearly impacts operation at high discharge voltage and further optimization which would aim at increasing the efficiency and reducing the discharge current oscillations. A new version of the PPS-Flex able to produce a strong magnetic field is presently under development, to continue the optimization procedure, and to start examining the discharge properties. The length of the ceramic cavity is a degree of freedom of which the impact remains to be investigated. The length could be decreased as ionization occurs behind the channel exit plane. This length must however be kept long enough to warrant homogenization of the injected gas.

Future efforts will be devoted to enhance the anode design, in order to mitigate thermal loads, for instance. The design of a dedicated wall-less Hall thruster will be the next logical step, after having the lessons learned from the testing of the last PPS-Flex version. This thruster design will fully exploit the possibilities offered by a wall-less architecture. The channel will be shortened, and the anode will be integrated in close proximity to the magnetic poles and might

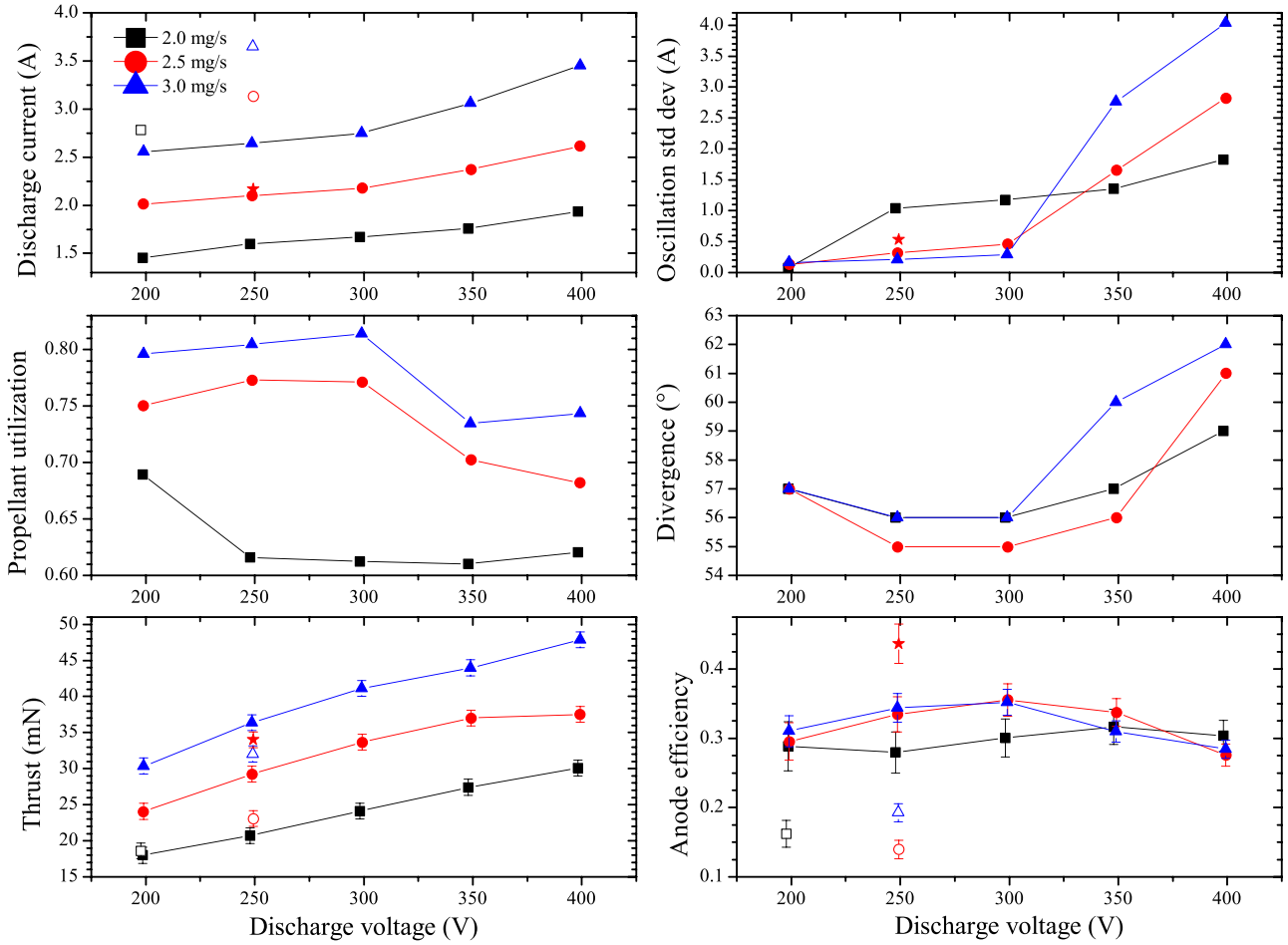

FIG. 3. Performance of the PPS-Flex in WL mode, at various operating points. The performance obtained with the PPS-FLEX in magnetic shielding-type (open symbols) and SPT100-type (star symbols) topologies are shown for comparison. From left to right, and top to bottom: discharge current mean value, standard deviation of the discharge current oscillation, ionization efficiency, beam divergence half-angle, thrust, and anode efficiency. The error bars on the anode efficiency have been estimated considering the thrust uncertainty only.

even be used to screen the magnetic circuit from the plasma. Finally, the magnetic circuit must be adapted to generate topologies suitable for using alternative propellants, and most importantly allowing a dual-mode operation, i.e., the capability of operating at high anode flow rate or high discharge voltage.

This study was performed within the framework of the CNRS/CNES/SNECMA/Universities joint-research program GIS entitled "Propulsion par plasma dans l'espace." J. Vaudolon benefits from a CNES-Snecma Ph.D. Grant.

[1]E. Ahedo, "Plasma for space propulsion," Plasma Phys. Controlled Fusion **53**(12), 124037 (2011).
[2]D. M. Goebel and I. Katz, *Fundamentals of Electric Propulsion* (Wiley, 2008).
[3]V. V. Zhurin, H. R. Kaufmann, and R. S. Robinson, "Physics of closed drift thrusters," Plasma Sources Sci. Technol. **8**, R1 (1999).
[4]K. Dannenmayer and S. Mazouffre, "Elementary scaling relations for Hall effect thrusters," J. Propul. Power **27**, 236 (2011).
[5]S. Mazouffre, R. Pérez Luna, and K. Dannenmayer, "Examination of plasma-wall interactions in Hall effect thrusters by means of calibrated thermal imaging," J. Appl. Phys. **102**, 023304 (2007).
[6]S. Mazouffre, K. Dannenmayer, and C. Blank, "Impact of discharge voltage on wall-losses in a Hall thruster," Phys. Plasmas **18**, 064501 (2011).
[7]I. G. Mikellides, I. Katz, R. R. Hofer, D. M. Goebel, and K. DeGrys, "Magnetic shielding of the channel walls in a Hall plasma accelerator," Phys. Plasmas **18**, 033501 (2011).
[8]I. G. Mikellides, I. Katz, R. R. Hofer, and D. M. Goebel, "Magnetic shielding of walls from the unmagnetized ion beam in a Hall thruster," Appl. Phys. Lett. **102**, 023509 (2013).
[9]I. G. Mikellides, I. Katz, R. R. Hofer, and D. M. Goebel, "Magnetic shielding of a laboratory Hall thruster. I. Theory and validation," J. Appl. Phys. **115**, 043303 (2014).
[10]R. R. Hofer, D. M. Goebel, I. G. Mikellides, and I. Katz, "Magnetic shielding of a laboratory Hall thruster. II. Experiments," J. Appl. Phys. **115**, 043304 (2014).
[11]D. M. Goebel, R. R. Hofer, I. G. Mikellides, I. Katz, J. E. Polk, and B. Dotson, "Conducting wall Hall thrusters," in *Proceedings of the 33rd IEPC, Washington, DC* (2013), p. IEPC 2013-276.
[12]S. Mazouffre, J. Vaudolon, G. Largeau, C. Hénaux, A. Rossi, and D. Harribey, "Visual evidence of magnetic shielding with the PPS-FLEX Hall thruster," IEEE Trans. Plasma Sci. **42**, 2668–2669 (2014).
[13]S. Mazouffre, S. Tsikata, and J. Vaudolon, "Development and characterization of a wall-less Hall thruster," J. Appl. Phys. **116**, 243302 (2014).
[14]S. Mazouffre, J. Vaudolon, S. Tsikata, G. Largeau, C. Hénaux, D. Harribey, A. Rossi, J. Gonzalez del Amo, A. Bulit, and K. Dannenmayer, "Optimization of magnetic field topology and anode geometry for a wall-less Hall thruster," in *Proceedings 51st Joint-Propulsion Conference, Cleveland, Ohio* (2015), p. AIAA 2015-4007.
[15]S. Mazouffre, G. Bourgeois, J. Vaudolon, L. Garrigues, C. Hnaux, D. Harribey, R. Vilamot, A. Rossi, S. Zurbach, and D. Le Mhaut, "Development and testing of Hall thruster with flexible magnetic field configuration," J. Propul. Power **31**, 1167–1174 (2015).
[16]L. Garrigues, S. Mazouffre, C. Hénaux, R. Vilamot, A. Rossi, D. Harribey, G. Bourgeois, J. Vaudolon, and S. Zurbach, "Design and first test campaign results with a new flexible magnetic circuit for a Hall thruster," in

Proceedings of the 33rd International Electric Propulsion Conference (2013), p. IEPC 2013-250.
[17]S. Mazouffre, P. Echegut, and M. Dudeck, "A calibrated infrared imaging study on the steady state thermal behavior of Hall effect thrusters," Plasma Sources Sci. Technol. **16**, 13–22 (2007).
[18]J. P. Boeuf and L. Garrigues, "Low frequency oscillations in a stationnary plasma thruster," J. Appl. Phys. **84**, 3541 (1998).
[19]E. Y. Choueiri, "Plasma oscillations in Hall thrusters," Phys. Plasmas **8**, 1411 (2001).
[20]J. Kurzyna, S. Mazouffre, A. Lazurenko, L. Albarde, G. Bonhomme, K. Makowski, M. Dudeck, and Z. Peradzynski, "Spectral analysis of Hall-effect thruster plasma oscillations based on the empirical mode decomposition," Phys. Plasmas **12**, 123506 (2005).